DEUTSCHES ELEKTRONEN-SYNCHROTRON **DESY**

DESY 89-078
June 1989

Strategies for Directly Observing Particle-Antiparticle Oscillations in the $B_s^0 - \overline{B}_s^0$ system

H. Steger

Deutsches Elektronen-Synchrotron DESY

ISSN 0418-9833

NOTKESTRASSE 85 · 2 HAMBURG 52

To be sure that your preprints are promptly included in the HIGH ENERGY PHYSICS INDEX , send them to the following address (if possible by air mail) :

DESY
Bibliothek
Notkestrasse 85
2 Hamburg 52
Germany

DESY 89-078
June 1989

ISSN 0418-9833

Strategies for Directly Observing Particle-Antiparticle Oscillations in the B_s^0-$\overline{B_s^0}$ System*

Herbert Steger
Deutsches Elektronen Synchrotron - DESY
Hamburg, Fed. Rep. Germany

ABSTRACT

Time dependent methods for determining the mixing parameter x_s in the B_s system are of special interest, particularly for as large values of x_s as expected in the standard model. Here we concentrate on the situation just above the threshold for $B_s^*\overline{B_s^*}$ production at an asymmtetric e^+e^- collider. Two methods are considered: the same sign dilepton distribution without any further tag, and the case where one tags on D_s mesons in addition in order to reduce the background. It turns out that an accuracy of 10% in the quantity $\Delta|t_1 - t_2|/\tau$ is of crucial importance in both cases. With a number of about 5×10^6 $b\bar{b}$ quark pairs such measurements could be sensitive to values of x_s up to 15.

* invited talk given at the 24th Recontres de Moriond

1. Introduction

In the standard model of electroweak interactions the entries of the fermion mass matrix are free parameters. In order to find the deeper origin of these parameters, it is obviously very important to restrict their allowed ranges by experiment as tightly as possible. The recent observation of B_d^0-$\overline{B_d^0}$ mixing by ARGUS [1] and CLEO [2] has far reaching consequences in this respect. In the three family standard model, its unexpectedly large magnitude implies, for example, an increased lower bound on the top quark mass [3] and, at the same time leads to improved bounds on the Cabibbo-Kobayashi-Maskawa (CKM) matrix elements [4].

Let us recall some basic facts: It is convenient to parametrize the CKM matrix according to Maiani and Wolfenstein [5],

$$V = \begin{pmatrix} 1-\frac{1}{2}\lambda^2 & \lambda & A\rho\lambda^3\epsilon^{-i\delta} \\ -\lambda & 1-\frac{1}{2}\lambda^2 & A\lambda^2 \\ A\lambda^3(1-\rho e^{i\delta}) & -A\lambda^2 & 1 \end{pmatrix} , \qquad (1)$$

where $\lambda = 0.22$ is the Cabibbo angle and the parameters $A = 1.05 \pm .17$ and $\rho \leq 0.9$ are obtainable from B decay. The allowed range for the phase δ is restricted by the parameter ϵ of CP violation in the K^0-$\overline{K^0}$system and the mixing parameter $x_d = 0.73 \pm 0.13$ in the system of neutral B_d mesons. Figs 1 and 2 are taken from Ref [4], where we analyzed the presently allowed ranges in the ρ-δ plane and possible restrictions by measuring certain CP violating asymmetries. In Fig 1 we show the allowed domain for for fixed values of m_t (= 60,90,120 and 180GeV), and in Fig 2 the full range which contains areas of fixed x_s. As one can easily see, combinig direct measurements of m_t and x_s would considerably reduce the presently existing freedom.

A problem arises, however, because with $x_d \sim 0.7$ the three family standard model predicts rather large values of x_s. One finds:

$$\frac{x_d}{x_s} \geq |\frac{V_{ts}}{V_{td}}|^2 = \lambda^2 \left(1 + \rho^2 - 2\rho\cos\delta\right) , \qquad (2)$$

and therefore gets as a conservative lower bound $x_s \geq 3$ [6]. In Ref [7] we discussed various methods for obtaining the quantity x_s experimentally. Special emphasis was put on the question of what accuracy is necessary for achieving a further reduction of the allowed area in the standard model parameter space. One result was that time integrated methods are not likely to give more information on x_s than the presently known limit. This is because the observables involved behave at best like $1 + O(1/x_s^2)$ for large x_s. Since with time dependent methods the period of oscillation is given by $T = \frac{2\pi\tau}{x_s}$ (τ = proper lifetime), these appear much more promising. It is clear, that because of the short lifetime of B mesons, a large boost is necessary so that the b and $\bar{b}$ quarks are produced with large

momenta in the laboratory system, and in this way their decay paths become visible. In principle there are two possibilities for such experiments—either at energies high above the threshold for $B_s\overline{B_s}$ production or at an asymmetric e^+e^- collider at a CM energy near the $\Upsilon(5s)$ mass. Here we concentrate on the latter method and discuss the background contributions and systematic errors. Using these ingredients as input we produce decay time histograms to which afterwards a fitting routine is applied. In this analysis we ignore CP violating effects and lifetime differences in B decays.

2 Oscillations near the $B_s^0\ \overline{B_s^0}$ Threshold

Due to mixing, the interaction and mass eigenstates of B_s mesons do not coincide:

$$B_{\mathrm{H,L}} = \frac{1}{\sqrt{1+|\eta|^2}}(B_q \pm \eta\overline{B_q})\ , \tag{3a}$$

where

$$\eta = \sqrt{\frac{M_{12}^* - \frac{i}{2}\Gamma_{12}^*}{M_{12} - \frac{i}{2}\Gamma_{12}}}\ . \tag{3b}$$

In the cases B_d and B_s η is practically a pure phasefactor. Mixing can be observed as oscillations (as a function of proper time) in the number of decays to final states accessible only for the weak eigenstate B_s^0 but not for $\overline{B_s^0}$ (or vice versa):

$$\begin{aligned} |B_s(t)> &= f_+(t)|B_s(0)> + \eta f_-(t)|\overline{B_s}(0)> \\ |\overline{B_s}(t)> &= f_+(t)|\overline{B_s}(0)> + \frac{1}{\eta}f_-(t)|B_s(0)>\ , \end{aligned} \tag{4a}$$

where

$$f_\pm = \exp(-i(\mathrm{M} - \frac{i}{2}\Gamma))\frac{1}{2}\{\exp(-i\frac{x_s}{2}\frac{t}{\tau}) \pm \exp(i\frac{x_s}{2}\frac{t}{\tau})\}\ , \tag{4b}$$

and $x_s = \Delta \mathrm{M_{B_s}}/\Gamma_{\mathrm{B_s}}$. The oscillation period then is determined by x_s and τ. At energies around the mass of $\Upsilon(5s)$ B_s mesons can only be produced in the initial state $B_s^0\overline{B_s^0}$, or from the decays of the excited states $B_s^*\overline{B_s}$, $B_s\overline{B_s^*}$, or $B_s^*\overline{B_s^*}$. In any case the $B_s^0\overline{B_s^0}$ pair is produced in a definite state of C parity in the $B^0\overline{B^0}$ CM frame. The decay time distributions for definite C parity of the $B_s^0\overline{B_s^0}$ system show the following dependence on the proper times t_1 and t_2 :

$$N(B_s^0\overline{B_s^0} \to B_s^0\overline{B_s^0}; t_1, t_2) \sim \exp(-\frac{t_1+t_2}{\tau}) \begin{cases} \cos^2(\frac{x_s}{2}\frac{t_1+t_2}{\tau}), & \text{for } C=+1\ ; \\ \cos^2(\frac{x_s}{2}\frac{t_1-t_2}{\tau}), & \text{for } C=-1\ . \end{cases} \tag{5a}$$

$$\begin{aligned} N(B_s^0\overline{B_s^0} \to B_s^0B_s^0; t_1, t_2) + N(B_s^0\overline{B_s^0} \to \overline{B_s^0}\,\overline{B_s^0}; t_1, t_2) \\ \sim \exp(-\frac{t_1+t_2}{\tau}) \begin{cases} \sin^2(\frac{x_s}{2}\frac{t_1+t_2}{\tau}), & \text{for } C=+1\ ; \\ \sin^2(\frac{x_s}{2}\frac{t_1-t_2}{\tau}), & \text{for } C=-1\ . \end{cases} \end{aligned} \tag{5b}$$

In the $\Upsilon(5s)$ CM system the $B_s\overline{B_s}$ pair is produced almost at rest. If an asymmetric e^+e^- collider is used to give the whole system a boost which is large enough to measure decay lengths, the energy of the B's is known approximately. The beam interaction point, however, is not, so that t_1 and t_2 cannot be individually measured. The $B_s^0\ \overline{B_s^0}$ proper time difference, on the other hand, is an accessible quantity. Integrating Eq (5) with respect to $t_1 + t_2$, while keeping $t_1 - t_2$ fixed, results in the following distributions in $|t_1 - t_2|$:

$$\begin{aligned} &N(B_s^0\overline{B_s^0} \to B_s^0\overline{B_s^0}; |t_1 - t_2|) \sim \\ &\frac{1}{2}\exp(-\frac{|t_1-t_2|}{\tau}) \begin{cases} \frac{1}{1+x_s^2}\{2\cos^2(\frac{x_s}{2}\frac{t_1-t_2}{\tau}) + x_s^2 - x_s\sin\{x_s\frac{|t_1-t_2|}{\tau})\}, & C=+1\ , \\ 2\cos^2(\frac{x_s}{2}\frac{t_1-t_2}{\tau}), & C=-1\ . \end{cases} \end{aligned} \tag{6a}$$

$$\begin{aligned} &N(B_s^0\overline{B_s^0} \to B_s^0B_s^0; |t_1 - t_2|) + N(B_s^0\overline{B_s^0} \to \overline{B_s^0}\,\overline{B_s^0}; t_1 - t_2) \sim \\ &\frac{1}{2}\exp(-\frac{|t_1-t_2|}{\tau}) \begin{cases} \frac{1}{1+x_s^2}\{2\sin^2(\frac{x_s}{2}\frac{t_1-t_2}{\tau}) + x_s^2 + x_s\sin(x_s\frac{|t_1-t_2|}{\tau})\}, & C=+1\ , \\ 2\sin^2(\frac{x_s}{2}\frac{t_1-t_2}{\tau}), & C=-1\ . \end{cases} \end{aligned} \tag{6b}$$

As suggested by Feldman [8], these two different classes of distributions can be observed as oscillations in the number of opposite and same sign dileptons. The big advantage of using semileptonic decays lies in their large branching fraction(12% for $B \to l\nu X$) and good detection efficiencies. These signals will be on top of a background coming from semileptonic B_d and $B^\pm$ decays. While charged B decays cause a purely exponential background, the contribution due to neutral $B_d^0\ \overline{B_d^0}$ decays carries a large oscillation period. Moreover, for both the B_s and B_d component one does not distinguish between the two different C parity eigenstates. Since the mass splitting between B_s and B_d is expected to be close to the $D_s - D$ mass difference, and since the hyperfine splitting in the B_s system is likely to be similar to the B_d system, we will take

$$\begin{aligned} \Delta \mathrm{m}_{B_s - B_d} &\simeq 100\mathrm{MeV}\ , \\ \Delta \mathrm{m}_{B_s^* - B_s} &\simeq 50\mathrm{MeV}\ . \end{aligned} \tag{7}$$

Therefore, $B_s\overline{B_s}$ pairs are always accompanied by $B_d\overline{B_d}$, $B_d\overline{B_d^*}$, $B_d^*\overline{B_d}$ and $B_d^*\overline{B_d^*}$ pairs. Since the mass of the $\Upsilon(5s)$ is 310 MeV + $2m_{B_d}$, pairs of $B_s\overline{B_s^*}$ ($B_s^*\overline{B_s}$) are also expected to be produced. However, $\Upsilon(5s)$ might not be heavy enough to decay into $B_s^*\ \overline{B_s^*}$. In Table 1 we show the ratios of probabilities for the decay of $\Upsilon(5s)$ into various states for two potential model calculations [9, 10]. In the first row, the mass of the $\Upsilon(5s)$ is assumed to be smaller than $2m_{B_s^*}$. The following two rows assume that $B_s^*\ \overline{B_s^*}$ can be produced.

Table 1

	$B_d^*\overline{B_d^*}$	$B_s^*\overline{B_s^*}$	$B_d\overline{B_d^*}$ + c.c.	$B_s\overline{B_s^*}$ + c.c.	$B_d\overline{B_d}$	$B_s\overline{B_s}$
BH*I* [9]	1	—	0.41	0.34	0.03	0.004
BH*II* [9]	1	0.67	0.41	0.18	0.03	0.004
CUSB [10]	1	1.18	1.34	0.1	0.67	0.21

Since for $C = +1$ (in contrast to $C = -1$) the distributions Eq (6) show a suppression of the oscillating part compared to the pure exponential, the CM energy should be adjusted to a value for which $C = -1$ B_s states predominate. In principle this value could be below the $B_s\overline{B_s^*} + c.\,c.$ threshold. However, this energy corresponds to a dip in the e^+e^- cross section. So, clearly energies around the $\Upsilon(5s)$ would be better suited (maybe slightly above if $2m_{B_s^*} > m_{\Upsilon(5s)}$).

As at the $\Upsilon(4s)$, there is the contribution of charged B^+B^- pairs to the opposite sign dileptons. Its weight relative to that due to $B_d^0\overline{B_d^0}$ pairs is given by the quantity λ which is a straightforward generalization of the one used by ARGUS [1]:

$$\lambda = \frac{Br(\Upsilon \to B^+B^-)}{Br(\Upsilon \to B_d^0\overline{B_d^0})}\ , \tag{8}$$

where we have assumed equal semileptonic branching ratios for B_d^0 and B^+ decays, and states with $C = \pm 1$ are understood to be included in the numerator and in the denominator. The quantity λ is estimated to be in the range $1 - 1.5$, and taken to be 1.2 in our analysis. Finally $B\overline{B}$ pairs can be produced in association with charged or neutral π's . In analogy to Eq (8) we parametrize this contribution as ρ, defined by

$$\rho \equiv \frac{Br(\Upsilon \to B\overline{B}\pi)}{Br(\Upsilon \to B_d\overline{B_d})}\ , \tag{9}$$

where we have again assumed equal semi-leptonic branching ratios for B_d and B^+, and $C = \pm 1$ states are implicitly included in both numerator and denominator. It is possible to estimate the relative contributions of $B_d^0\overline{B_d^0}\pi^0$, $B^+B^-\pi^0$, and $B^+\pi^-\overline{B_d^0}$ to ρ as follows. First, in analogy to Eq (8), the ratio of $B^+B^-\pi^0$ production to $B_d^0\overline{B_d^0}\pi^0$ production is expected to be about λ. Secondly, due to isospin considerations, the contribution of $B_d^0\overline{B_d^0}\pi^0$ is four times smaller than that of $B^+\overline{B_d^0}\pi^- + c.c.$ Therefore we have

$$\begin{array}{ccccc} B^+B^-\pi^0 & : & B^+\overline{B_d^0}\pi^- + B^-B_d\pi^+ & : & B_d^0\overline{B_d^0}\pi^0 \\ \lambda & : & 4 & : & 1\ . \end{array} \tag{10}$$

In the following we assume ρ to be 1 since, apart from phase space, there seems to be no indication that the production of an extra pion would be suppressed. The π^0 modes will effectively increase the contributions of both B^+B^- and $B_d^0\overline{B_d^0}$ pairs. For the contributions with charged π's, however, one finds a new kind of distribution:

$$\begin{aligned} N(B^+\overline{B_d^0} \to B^+\overline{B_d^0}; t_1, t_2) &\sim \exp(-\frac{t_1+t_2}{\tau})\cos^2(\frac{x_d}{2}\frac{t_1}{\tau})\ , \\ N(B^+\overline{B_d^0} \to B^+B_d^0; t_1, t_2) &\sim \exp(-\frac{t_1+t_2}{\tau})\sin^2(\frac{x_d}{2}\frac{t_1}{\tau})\ , \end{aligned} \tag{11}$$

which, after integration over $t_1 + t_2$ and symmetrization with respect to the sign of $t_1 - t_2$, leads to the following expressions:

$$\begin{aligned} &N(B^+\overline{B_d^0} \to B^+\overline{B_d^0}; |t_1 - t_2|) \sim \\ &\frac{1}{4+x_d^2}\exp(-\frac{|t_1-t_2|}{\tau})\left\{3 + \frac{x_d^2}{2} + \cos(x_d\frac{|t_1-t_2|}{\tau}) - \frac{x_d}{2}\sin(x_d\frac{|t_1-t_2|}{\tau})\right\}\ , \end{aligned} \tag{12a}$$

$$\begin{aligned} &N(B^+\overline{B_d^0} \to B^+B_d^0; |t_1 - t_2|) \sim \\ &\frac{1}{4+x_d^2}\exp(-\frac{|t_1-t_2|}{\tau})\left\{1 + \frac{x_d^2}{2} - \cos(x_d\frac{|t_1-t_2|}{\tau}) + \frac{x_d}{2}\sin(x_d\frac{|t_1-t_2|}{\tau})\right\}\ , \end{aligned} \tag{12b}$$

Similar equations are obtained when the initial state is $B^-B_d^0\pi^+$. The process of the type (12a) contributes to the opposite sign dilepton signal, whereas the process of type (12b) affects the same sign dilepton rate.

Combining all these components with their appropriate weights, for example in the model BHII, results in the theoretical distribution [11]. There are, however, experimental errors which one has to take into account. First there is the possibility of charge misidentification. We assume this error to amount to 5% in total ($\simeq 2.5\%$ for each single lepton), but it turns out that this does not affect the shape of the distributions significantly.

Of special importance is a systematic error [10] due to the fact that $B\overline{B}$ pairs are not produced at rest in the center of mass system (i.e. the Doppler effect). The distance between the decay vertices of the two B mesons in the lab system is approximately given by*

$$d = c\gamma\beta(t_1 - t_2) + c\gamma\beta_{\rm cm}\cos(\theta_{\rm cm})(t_1 + t_2) + O(\beta_{\rm cm}^2)\ , \tag{13}$$

where $\beta_{\rm cm}$ is the velocity of the B mesons in the center of mass system, and $\theta_{\rm cm}$ denotes the polar angle with respect to the beam pipe at which this meson is emitted in the CM. Taking $\langle t_1 + t_2\rangle \simeq 2\tau$ and $\langle|\cos\theta_{\rm cm}|\rangle = 2/\pi$, this leads to a systematic error in $(t_1 - t_2)$ as extracted from d:

$$\left[\frac{\Delta(t_1-t_2)}{\tau}\right]_{\rm syst} \simeq \frac{4}{\pi}\frac{\beta_{\rm cm}}{\beta} \simeq 1.8\,\beta_{\rm cm}\ . \tag{14}$$

In the last step we have assumed a 12.5 GeV on 2.3 GeV collider configuration as proposed in Ref [12]. This Doppler effect affects different modes in different ways. For example, with the center of mass energy just above the threshold for $B_s^*\overline{B_s^*}$ production, one finds that $B_s\overline{B_s}$ pairs coming from the decays of $B_s^*\overline{B_s^*}$ have, on average, $\beta_{\rm cm} = 0.01$, while $B_s\overline{B_s}$

* This assumes that the B's are produced back to back in the CM system. In fact, because of B^* and $B\overline{B}\pi$ production, this is not the case. However, a more accurate estimate of this systematic error would require a detailed Monte Carlo simulation.

pairs produced directly have $\beta_{\rm cm} = 0.14$. For $B\overline{B}$ pairs originating from all the various angular momentum states, we have

$$\begin{array}{lc} & B_s^*\overline{B_s^*}\ ,\ B_s\overline{B_s^*}+B_s^*\overline{B}_s\ ,\ B_s\overline{B}_s\ ,\ B_d^*\overline{B_d^*}\ ,\ B_d\overline{B_d^*}+B_d^*\overline{B}_d\ ,\ B_d\overline{B}_d\ ,\ B_dB\pi \\ \beta_{\rm cm}: & 0.01\ ,\quad 0.10\quad ,\ 0.14\ ,\ 0.20\ ,\quad 0.22\quad ,\ 0.24\ ,\ 0.16 \end{array} \tag{15}$$

Since the beam energy is expected to be well controlled, the main source of statistical error in $\frac{\Delta(t_1-t_2)}{\tau}$ is the finite vertex resolution. Assuming this resolution to be 25μm, one gets:

$$\left[\frac{\Delta(t_1-t_2)}{\tau}\right]_{\rm res} \simeq \frac{25\mu{\rm m}\cdot\sqrt{2}}{c\gamma\beta\tau} \simeq .1\ , \tag{16}$$

with the assumed asymmetric collider configuration ($\beta\gamma = 1$). An increase in the asymmetry of the beam energies leads to larger values of $\gamma\beta$ and therefore decreases the systematic uncertainty slightly. However, an increase in $\gamma\beta$ in Eq (16) will also result in an increased error in d, caused by the higher collimation of the B decay products. Therefore an optimal choice of the collider configuration might exist which would minimize $\left[\frac{\Delta(t_1-t_2)}{\tau}\right]_{\rm res}$. In the subsequent discussion we assume this minimal value to be given by Eq (16). We will, however, also consider larger values of the statistical error. This error sets the upper limit for the value of x_s accessible experimentally. We also note that, because of the systematic error, there is a minimum value of β required to measure x_s, i.e. there is a minimum necessary asymmetry in the beam energies.

In order to simulate this experimental situation we convolute the theoretical distributions (after taking into account 5% charge misidentification) with a Gaussian error factor. In this way one arrives at linear combinations of terms of the following form:

$$D(v) = \frac{1}{\sigma\sqrt{2\pi}}\int_{-\infty}^{\infty} g(v')e^{-\frac{(v-v')^2}{2\sigma^2}}dv'\ , \tag{17}$$

where σ is the experimental resolution, $v = \frac{|t_1-t_2|}{\tau}$, and $g(v)$ is one of

$$e^{-v}\ ,\quad e^{-v}\cos xv\ ,\quad e^{-v}\sin xv\ . \tag{18}$$

A straightforward calculation yields:

$$\begin{aligned} D_1(v,0) &= {\rm Re}(H_1(v,0)+H_2(v,0))\ , \quad \text{for } g(v)=e^{-v}\ , \\ D_1(v,x) &= {\rm Re}(H_1(v,x)+H_2(v,x))\ , \quad \text{for } g(v)=e^{-v}\cos xv\ , \\ D_2(v,x) &= {\rm Im}(H_1(v,x)+H_2(v,x))\ , \quad \text{for } g(v)=e^{-v}\sin xv\ . \end{aligned} \tag{19}$$

The functions $H_1(v,x)$ and $H_2(v,x)$ in the above equations are defined as follows:

$$\left.\begin{array}{l} H_1(v,x) \\ H_2(v,x) \end{array}\right\} = \frac{1}{2}e^{\frac{1}{2}\sigma^2(1-ix)^2}\mp v(1-ix)\left[1-{\rm erf}\left(\frac{\sigma^2\mp v}{\sqrt{2}\sigma}-i\frac{x\sigma}{\sqrt{2}}\right)\right]\ , \tag{20}$$

where ${\rm erf}(z)$ is the error function.

Finally histograms are generated by splitting the resulting continuous distributions into bins of size $\frac{|t_1-t_2|}{\tau} = .1$. The area of each of these bins is proportional to the number of events in the corresponding $\frac{|t_1-t_2|}{\tau}$ interval. Interpreting this number as a mean of the Poisson distribution, a random number is generated accordingly and taken to be the actual hight of the bin. As an example we show in Fig 3 histograms for same sign dilepton distributions for the scenarios BHII (a, c, e) and equal admixture (b, d, f) of all components (B_s, B_d, $C = \pm 1$) with $|\Delta(t_1-t_2)/\tau|_{\rm res} = .1$ and $x_s = 10$. Each case is presented for three different numbers of detected dilepton events: 2×10^4, 5×10^4 and 5×10^5. Taking into account semileptonic branching ratios, which give a factor $1/(.24)^2$ and allowing for finite experimental efficiency, the fact that some of the signal goes down the beam pipe and part of the events are lost by imposing a cut on the lepton energy in order to distinguish semileptonic B from D decays (an estimated combined factor of 8), these correspond to about 2×10^6, 5×10^6 and 5×10^7 initial $b\bar{b}$ quark pairs (at the $\Upsilon(5s)$). While in the BHII scenario the signal is evident with a number of only 5×10^4 detected dileptons, it seems to be hard to see it in the more pessimistic equal admixture case.

In order to make these statements more quantitative a least χ^2 fit using the MINUIT package was performed. In Fig 4a we show the best fit (dots and solid line) to the histogram (vertical bars give the size of the statistical error, horizontal bars the binsize) for $x_s = 10$ and a number of 5×10^4 detected dileptons. This is to be compared with the smooth dashed curve before randomization. The dots (and solid line) were found by fitting to the following four parameter function:

$$Fi(a_1,a_2,a_3,a_4,v) = \frac{1}{2}a_1(D_1(v,0)-a_2D_1(v,a_3)-a_4D_1(v,x_d))\ , \tag{21}$$

where $x_d = 0.7$ and a_3 should give the value of x_s searched for. The inclusion of a term proportional to $D_1(v,x_d)$ turns out to be important, since the contribution of $B_d^0\overline{B_d^0}$ decays cause a substantial deviation from an exponential behaviour which is modulated by some rapid oscillation. The results of the best fit are: $\chi^2 = 34.4$, $a_1 = 0.75\pm0.01$, $a_2 = 0.15\pm0.10$, $a_3 = x_s = 9.90\pm0.10$ and $a_4 = 0.60\pm0.02$. In Fig 4b we show the σ contour plots (up to five standard deviations) in the (a_1,x_s) plane. Finally in Fig 4c we explore the four dimensional parameter space by finding for each value of fixed $x_s = a_3$ the best fit in the remaining three parameters and plotting the obtained χ^2 against x_s. A very pronounced dip in χ^2 around $x_s = 10$ is clearly visible, and in addition one observes a steep rise in χ^2 for very low x_s. In the same way (taking the above as an ideal situation for measuring x_s) we analyzed the histograms for all kinds of combinations $\frac{\Delta|t_1-t_2|}{\tau}_{\rm res} = 10\%$, 20%, statistics of detected dileptons 2×10^4, 5×10^4 and 5×10^5 for the two scenarios considered in Fig 3. It seems possible to see up to $x_s = 15$ with $\frac{\Delta|t_1-t_2|}{\tau} = 10\%$ and

5×10^4 dileptons in scenario BHII, while still values up to around 10 might be reasonably well recovered for $\frac{\Delta|t_1-t_2|}{\tau} = 20\%$. With the same statistics and the equal admixture scenario $\frac{\Delta|t_1-t_2|}{\tau} = 20\%$ is sufficient to reach $x_s = 5$ while for $x_s = 10$ one definitely needs $\frac{\Delta|t_1-t_2|}{\tau} = 10\%$. It is interesting to see that in scenario BHII with $\frac{\Delta|t_1-t_2|}{\tau} = 10\%$ 2×10^4 detected dileptons still seem to be sufficient for identifying $x_s = 10$, whereas a statistics of 5×10^5 is not enough to see $x_s = 20$.

There have been suggestions to utilize a D_s tag in order to enhance the signal to background ratio and in this way manage with a smaller number of $b\bar{b}$ quark pairs, or to allow for a larger resolution error $\left[\frac{\Delta(t_1-t_2)}{\tau}\right]_{\rm res}$. In Fig 5a we show the histogram and best fit for 2000 reconstructed llD_s events (according to scenario BHII, 5% charge misidentification, $\frac{\Delta|t_1-t_2|}{\tau} = 10\%$ and the input value $x_s = 10$). Here the following two parameter function was used for the fit:

$$Fi(a_1, a_2, v) = a_1 Odd(a_2, v) + (1 - a_1) Even(a_2, v) \ , \qquad (22)$$

where *Odd* and *Even* are the Gaussian convoluted functions of Eq (6b), and a_2 should reproduce $x_s = 10$. For $\frac{\Delta|t_1-t_2|}{\tau} = 10\%$ one finds with quite low $\chi^2 = 15$ $a_1 = 0.81 \pm .22$ (input value was .79) and $a_2 = 10.24 \pm 0.11$. In Fig 5b we show the corresponding σ contour plot in the (a_2, x_s) plane. This does not look better than for the untagged dilepton distribution (assuming a reconstuction efficiency of 4% for D_s mesons 2000 detected llD_s events correspond to 50,000 detected ll events). In addition Fig 5c, showing the plot χ^2 vs x_s (now performing a one parameter least square fit for each fixed value of x_s), reveals that the distance of the minimum in χ^2 to the plateau is much smaller than in the untagged case. Repeating the same analysis but now with $\frac{\Delta|t_1-t_2|}{\tau} = 20\%$ one only finds an extremely shallow minimum in χ^2 around $a_2 = 10.9$ and no reasonable error bars. With 90% confidence level one might exclude $x_s \leq 3.5$ in this case, without getting any upper bound (in the BHII scenario). This seems to tell us two things: First, tagging on D_s mesons in addition to the dilepton pair does not look as rewarding as it might seem initially (this is because of the loss of a factor 25 in statistics). Secondly, the range of x_s reachable depends crucially on the overall resolution error $\frac{\Delta|t_1-t_2|}{\tau}$. In many cases it turned out that an improvement by a factor of 2 (from 10% to 20%) is much more rewarding than an increase of one order of magnitude in statistics.

3. Conclusions

Analyzing decay time distributions at asymmetric e^+e^- colliders near the $\Upsilon(5s)$ resonance we discussed the physics input necessary to find the range of x_s accessible and the number of initial $b\bar{b}$ quark pairs required. Same sign dilepton distributions turn out to yield the clearest signal. The loss in statistics caused by tagging on a D_s meson in addition invalidates the effect of increasing the signal to background ratio. As expected,

by using a fitting routine we find somewhat more optimistic upper values of x_s accessible with definite statistics and resolution error than by just inspecting the histograms [7]. So, assuming a vertex resolution of 25μm at least, a value of x_s up to 15 seems not to be out of reach with 5×10^6 $b\bar{b}$ pairs (10 for the equal admixture scenario).

Acknowledgements

I would like to thank P. Krawczyk and D. London for fruitful collaboration and T. Nakada for helpful discussions. Special thanks go to Tran Thanh Van and the organizers of this pleasant and stimulating meeting.

References

[1] ARGUS Collaboration: H. Albrecht et al, Phys. Lett. **192B** (1987) 245.

[2] CLEO Collaboration: A. Jawahery, *Proceedings of the XXIV International Conference on High Energy Physics*, Munich, W. Germany (1988).

[3] A. Ali, DESY preprint DESY 87-083 (1987); J. Donoghue, T. Nakada, E. Paschos and D. Wyler, Phys. Lett **195B** (1987) 285; J. Ellis, J. Hagelin and S. Rudaz, Phys. Lett. **192B** (1987) 201; I. I. Bigi and A. I. Sanda, Phys. Lett. **194B** (1987) 307; J. Maalampi and M. Roos, Phys. Lett. **195B** (1987) 489; V. Barger, T. Han, D. V. Nanopoulos and R. J. N. Phillips, Phys. Lett. **194B** (1987) 312; H. Harari and Y. Nir, Phys. Lett. **195B** (1987) 586; Y. Nir, SLAC preprint SLAC-PUB-4368, (1987); V. A. Khoze and N. G. Uraltsev, Leningrad preprint 1290, (1987); G. Altarelli and P. Franzini, Z. Phys. **C37** (1988) 271.

[4] P. Krawczyk, D. London, R. Peccei and H. Steger, Nucl. Phys. **B307** (1988) 19.

[5] L. Maiani, Phys. Lett. **62B** (1976) 183; L. Wolfenstein, Phys. Ref. Lett. **51** (1983) 1945.

[6] G. Altarelli and P. Franzini, Z. Phys. **C37** (1988) 271.

[7] P. Krawczyk, D. London and H. Steger, DESY preprint, DESY 88-163 (1988).

[8] This suggestion was made by G. Feldman at Snowmass '88.

[9] N. Byers and D. S. Hwang, *Proceedings of the Workshop on High Sensitivity Beauty Physics at Fermilab*, ed. A. J. Slaughter, N. Lockyer, and M. P. Schmidt (Fermi National Accelerator Laboratory, Batavia, 1987) p. 199.

[10] J. Lee-Franzini, SUNY preprint Print-88-047 (Stony Brook) (1988).

[11] For further literature on potential model calculations see: A. D. Martin and C.-K. Ng, Z. Phys **C40** (1988) 133; S. Ono, A. I. Sanda and N. A. Törnqvist, Phys. Rev. **D38** (1988) 1619.

[12] R. Aleksan, J. E. Bartelt, P. Burchat, and A. Seiden, SLAC preprint SLAC-PUB-4673 (1988).

Figure Captions

Fig 1: The domain in ρ-δ space (δ in radians), within which the standard model is compatible with the measurements of ϵ and x_d (90% c.l.). B_K and f_B are allowed to vary within the ranges $1/3 \leq B_K \leq 1$ and 100 MeV $\leq (f_B)^{1/2} \leq$ 200 MeV.
a) The areas 1, 2, 3, 4 correspond to fixed values $m_t = 60, 90, 120, 180$ GeV, respectively.

Fig 2: As in Fig 1, but now all three parameters m_t, $(f_B)^{1/2}$ and B_K are varied: 40 GeV $\leq m_t \leq$ 180 GeV, 100 MeV $\leq (f_B)^{1/2} \leq$ 200 MeV and $1/3 \leq B_K \leq 1$. In addition, the further restrictions by fixed $x_s = 3, 7, 15$ are shown.

Fig 3: Simulation of the actual experimental data for the same sign dilepton distribution with $x_s = 10$ for the two scenarios BHII (a,c,e) and equal mixture (b,d,f), with $\left[\frac{\Delta(t_1-t_2)}{\tau}\right]_{\rm res} = 0.1$, and 2×10^4 (a,b), 5×10^4 (c,d), 5×10^5 (e,f) reconstructed dileptons.

Fig 4: Best fit to the histogram Fig 3c ($x_s = 10$, 5×10^4 reconstructed dileptons, BHII).
a) The histogram is given by the crosses, where vertical bars give the size of the statistical error and horizontal bars the binsize. The best fit consists in the dots and the solid curve. This is to be compared with the smooth dashed curve, from which the histogram is produced via application of our randomization procedure.
b) The σ contour plot up to five standard deviations in the plane of the fitting parameters a_2 and $a_3 = x_s$.
c) χ^2 of the best fit (for fixed values of x_s) versus x_s.

Fig 5: Like Fig 4, but now for 2000 reconstructed llD_s events, using again $x_s = 10$, scenario BHII, and 5% charge misidentification and $\frac{\Delta|t_1-t_2|}{\tau} = 10\%$.
a) The best fit,
b) the σ contour plot in the plane of fitting parameters a_1, and $a_2 = x_s$,
c) like Fig 4c, χ^2 of the best fit (for fixed values of x_s) versus x_s.

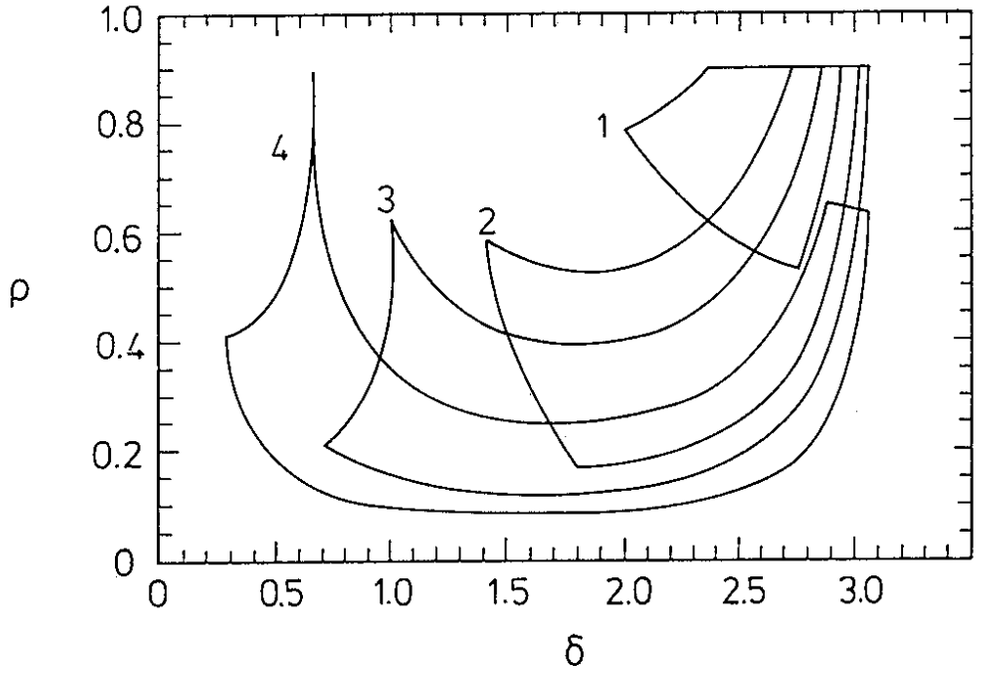
1.0
0.8
0.6
0.4
0.2
0
ρ
0
0.5
1.0
1.5
2.0
2.5
3.0
δ
1
2
3
4

Fig 1

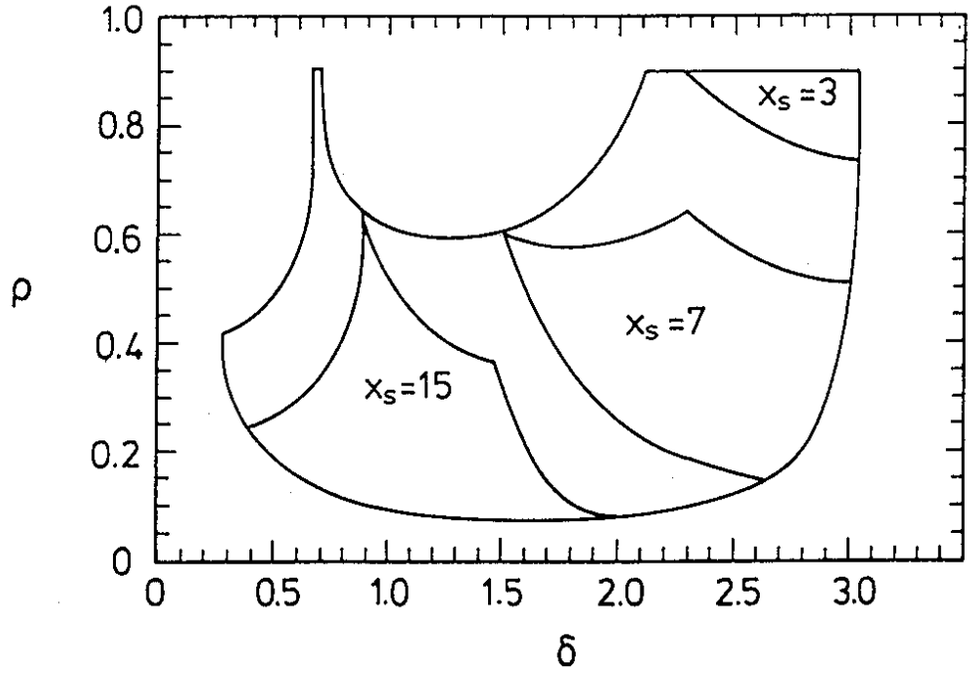
1.0
0.8
0.6
0.4
0.2
0
ρ
0
0.5
1.0
1.5
2.0
2.5
3.0
δ
x_s =3
x_s =7
x_s=15

Fig 2

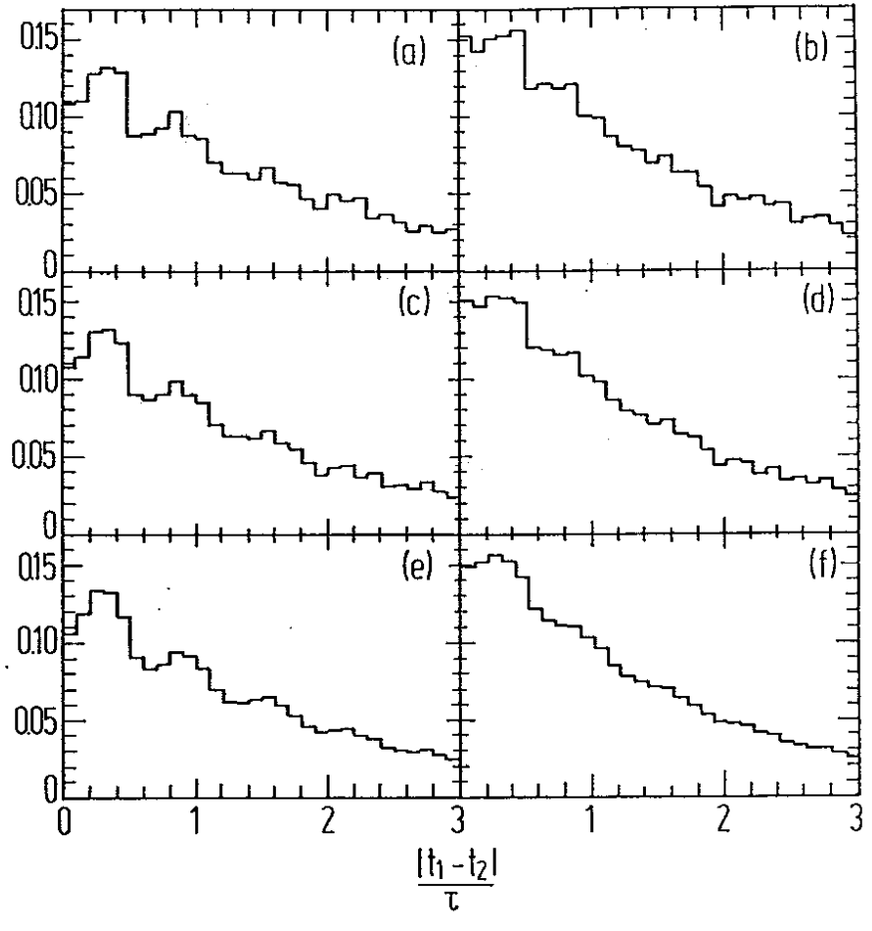
(a)
(b)
(c)
(d)
(e)
(f)
0.15
0.10
0.05
0
0
1
2
3
$\frac{|t_1 - t_2|}{\tau}$

Fig 3

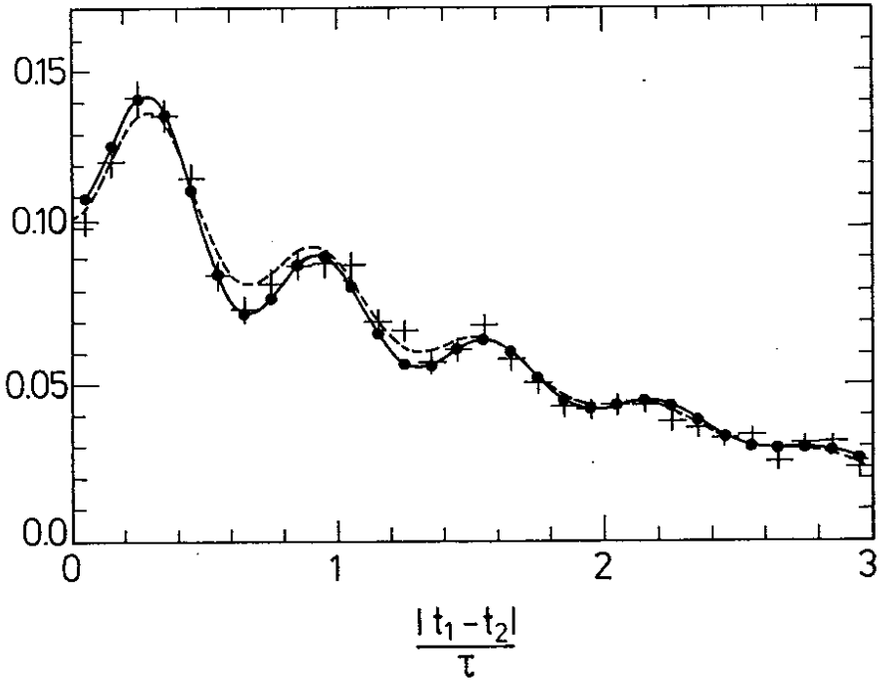
0.15
0.10
0.05
0.0
0
1
2
3
$\frac{|t_1 - t_2|}{\tau}$

Fig 4a

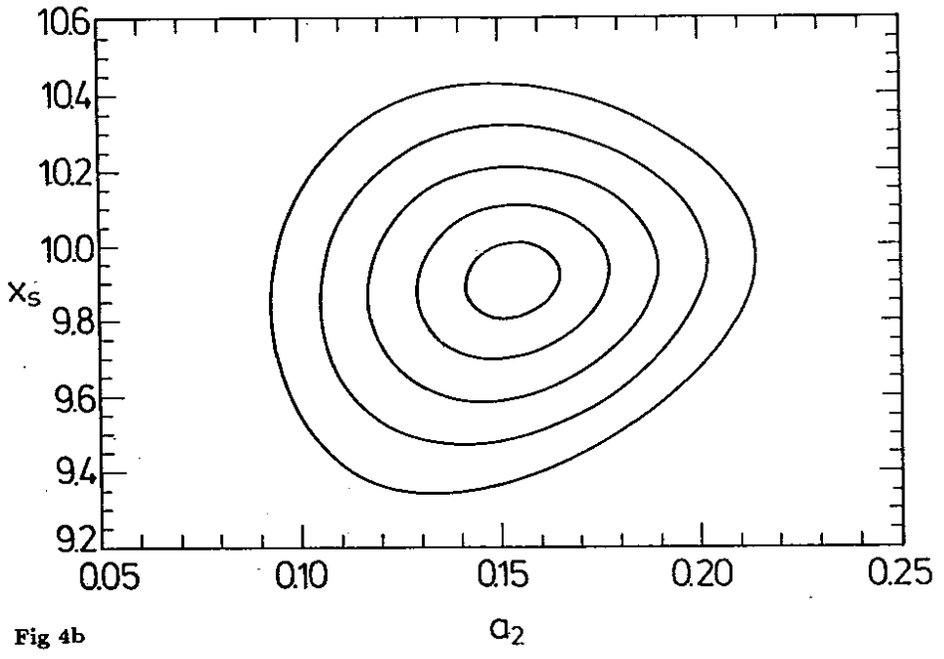

Fig 4b

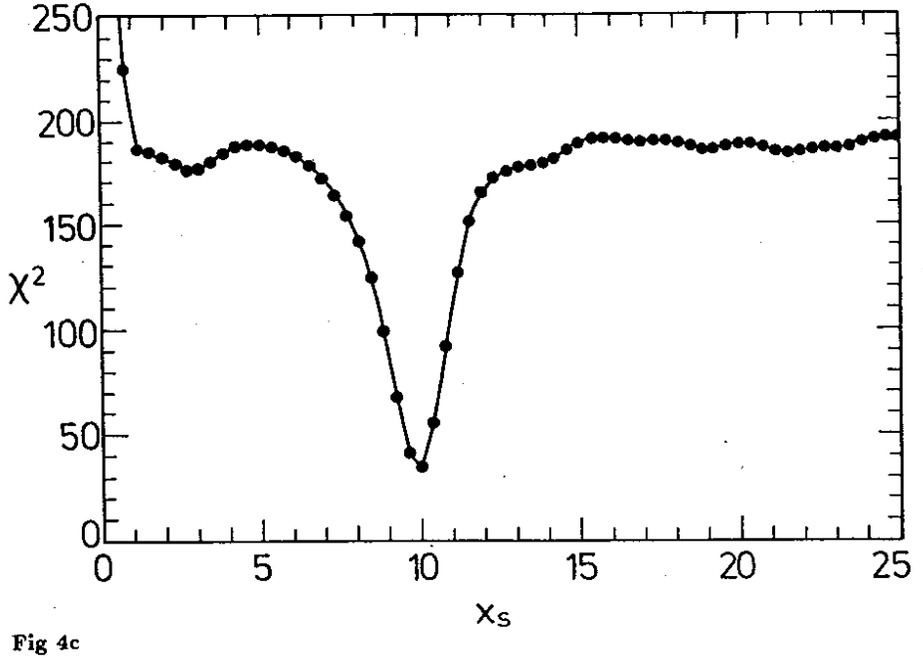

Fig 4c

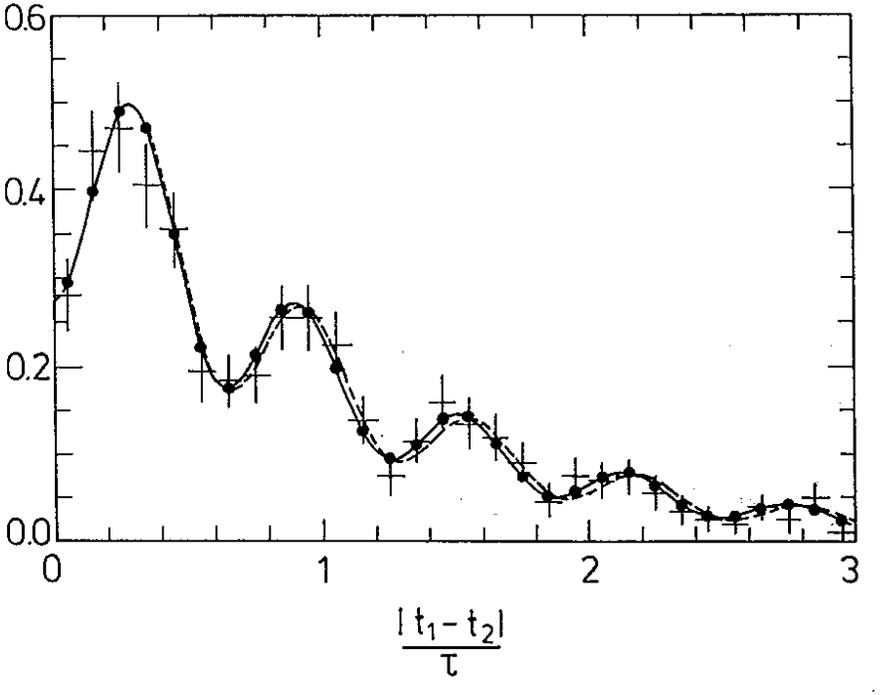

Fig 5a

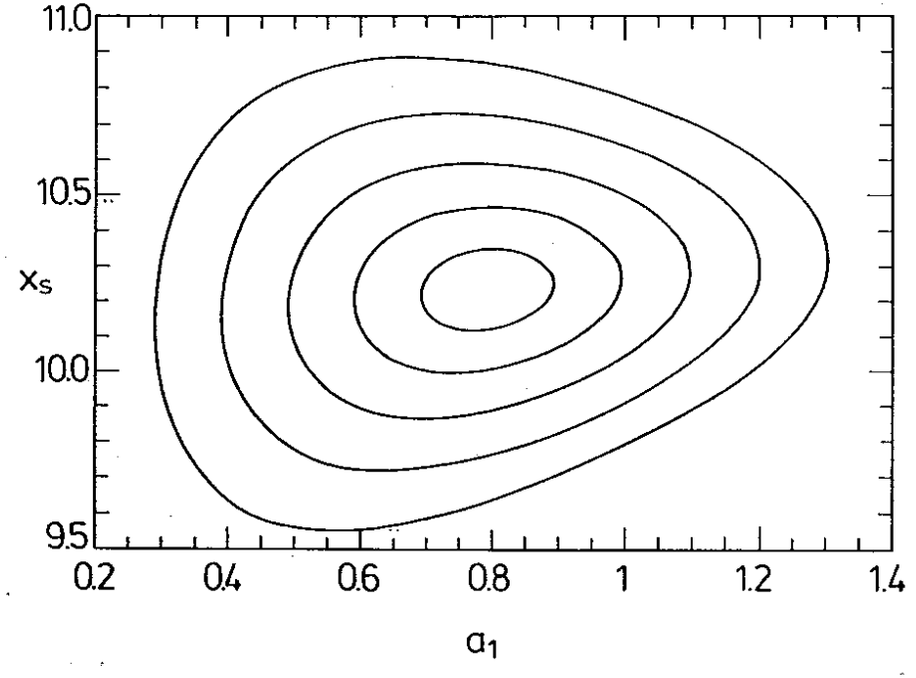
11.0
10.5
10.0
9.5
x_s
0.2
0.4
0.6
0.8
1
1.2
1.4
a_1

Fig 5b

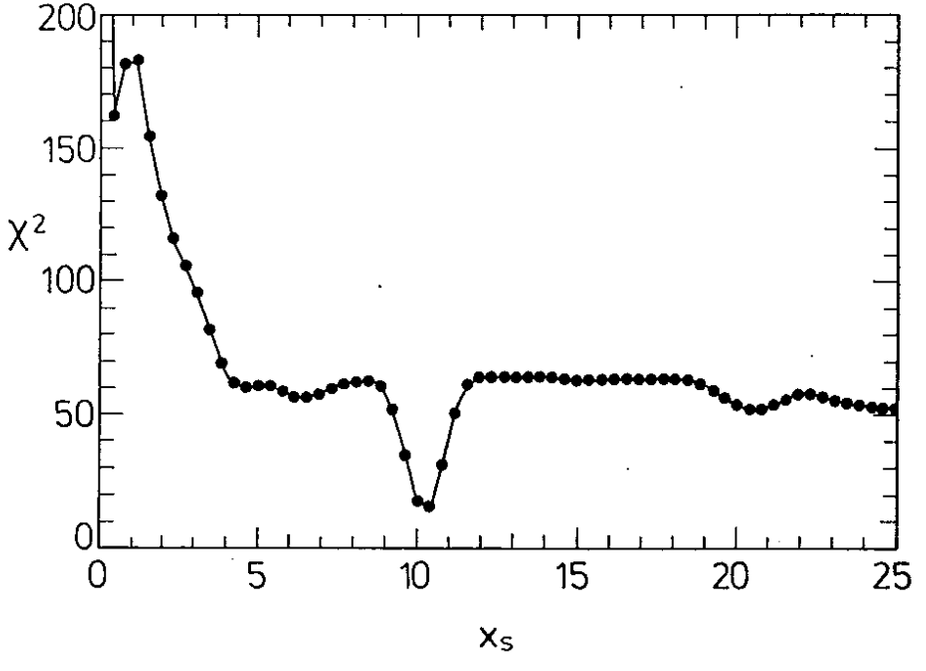
200
150
100
50
0
χ^2
0
5
10
15
20
25
x_s

Fig 5c